Proceedings World Geothermal Congress 2020+1
Reykjavik, Iceland, April - October 2021

Secondary Mineralogy Associated with Supercritical Fluid Formation at Magmatic-Geothermal Contact Zone

Matylda Heřmanská, Barbara I. Kleine, Andri Stefánsson

University of Iceland, Sturlugata 7, Reykjavik 101, Iceland

mattylda@hi.is

Keywords: Geothermal, secondary mineralogy, supercritical fluids, geochemical modeling, flow-through experiment

ABSTRACT

An increasing energy demand prompts exploration of high-temperature and supercritical resources associated with intrusion-based geothermal systems. Utilization of such fluids may lead to an increase in power production. However, the presence of supercritical fluids is associated with formation of mineral deposits that can potentially jeopardize the utilization of the supercritical reservoir. The formation of such deposits is yet poorly constrained. Here, we studied the effects of reservoir parameters such as boiling temperature or fluid source composition on secondary mineralogy upon supercritical fluid formation. For this purpose, four flow-through experiments with varying inlet fluid compositions were carried out at supercritical conditions. The experimental findings were subsequently compared with geochemical modeling results. The experimental and modeling results revealed that the types of mineral deposits formed upon supercritical fluid formation were dependent on fluid source composition, pH and boiling temperature. In low-NaCl high-temperature geothermal systems, conductive heating and boiling of subcritical fluids to supercritical conditions may result in the formation of alteration sequences consisting of Fe-Mg-Al silicates (clays or chlorites), Na-K feldspar, wollastonite, quartz and minor amounts of salt. At boiling temperature above 250 °C, the amount of precipitates may be twenty times larger than in geothermal systems with boiling temperature below 200 °C. In high-NaCl high-temperature geothermal systems, the amount of secondary minerals forming may be sixty times larger than in geothermal systems with boiling temperature below 200 °C, and three times larger than in low-NaCl high-temperature geothermal systems. Surprisingly, mineral amounts precipitating in high-temperature geothermal systems with elevated HCl concentrations may be as large as in low-NaCl geothermal systems. However, the highly acidic character in such systems favors precipitation of salts and silica into silica gel structures. This could potentially contribute to scaling and corrosion observed in some high-temperature geothermal wells, such as the IDDP-1 well in Krafla (Iceland).

1. SUPERCRITICAL FLUID FORMATION IN ACTIVE GEOTHERMAL SYSTEMS

Exploration of supercritical fluids associated with intrusion-related geothermal systems may increase power production by geothermal energy. So far, more than 90 % of the power production from geothermal systems is produced by high-temperature fields (Rivera-Diaz et al. 2016). Power production of one high-temperature well generally corresponds to 5-10 MW. This is ten times lower than potential power production of a well that would discharge supercritical fluids (Friðleifsson et al. 2014).

Supercritical fluids have been reported from active high-temperature geothermal systems associated with plate boundaries and magmatic intrusions located in < 6 km depth (Stimac et al. 2015). Supercritical fluids most likely form at an early stage in the evolution of a geothermal system within the magmatic-geothermal contact zone (Fig. 1; Scott et al., 2016). Upon cooling of a magmatic intrusions, convecting subcritical meteoric water or seawater may reach supercritical temperatures of >400 °C within the magmatic-geothermal contact zones due to conductive heating of the surrounding rocks and groundwater by the magmatic heat source (Heřmanská et al., 2019).

When fluids heat beyond the critical point of water, their composition may change abruptly as the physical properties of the fluid components change at the two-phase (liquid and vapor) and supercritical fluid phase boundary (Fournier and Potter 1982; Manning 1994; Dolejš and Manning 2010). In general, the concentration of mineral-forming elements (e.g., Si, Al, Mg, Ca) increases with temperature at subcritical conditions. At the two-phase and supercritical fluid phase boundary, however, progressive boiling and an accompanying increase of specific enthalpy in the fluid phase may lead to a sudden decrease in solubility of these elements resulting in the precipitation of silica deposits upon supercritical fluid formation. Components with lower boiling points or non-reactive elements partition into the vapor, and therefore their concentrations are not affected by boiling (Simonson and Palmer 1993). This group involves volatile elements, such as carbon (in form of CO_2) or sulphur (in form of H_2S), B and possibly Cl.

Here, we investigate the alteration mineralogy associated with supercritical fluid formation. In addition, we explore the effects of fluid source composition on the alteration sequence and associated changes in the host rock permeability at the magmatic-geothermal contact zone. For this purpose, we carried out high-temperature flow-through experiments with varying inlet solution compositions. The fluid compositions used in the experiments correspond to fluid types reported from rift-zone related (low NaCl fluids) and subduction-related (elevated or high NaCl, volatile rich fluids) geothermal systems. The experimental results were further compared to results obtained from geochemical modelling to identify the processes that were responsible for the observed changes in mineralogy.

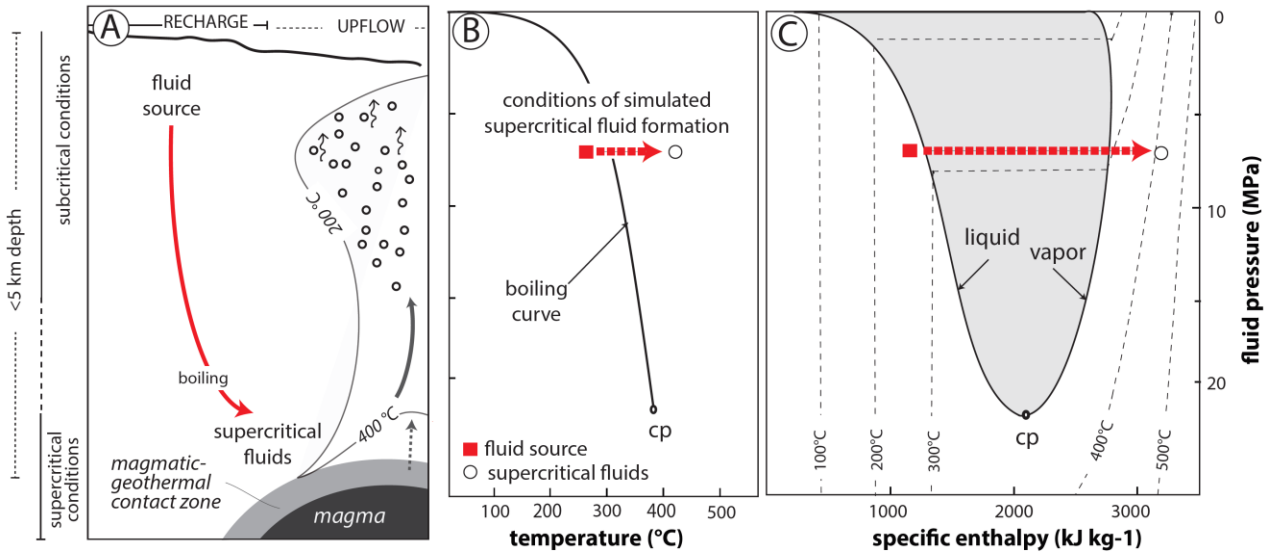

Figure 1: Main features and fluid phase relations in volcanic high-geothermal system. A) Conceptual view of a geothermal system with focus on the magmatic-geothermal contact zone, with highlighted p-t-h paths of supercritical fluid formation (in red), magma gas addition (black dashed arrow) and supercritical fluid condensation (thick black arrow). (B) The boiling curve of water. (C) The phase diagram of water showing pressure, enthalpy and temperature relations. P-t-h conditions of high-temperature experiment and geochemical modeling presented in this study are shown by red arrow.

2. METHODS

2.1 High-temperature experiment and chemical analysis

Here, we use reservoir conditions of supercritical fluid formation presented by Scott et al. (2015, 2016) to design the experimental set-up. To understand the importance of source fluid composition on secondary mineral formation, we carried out simulations for conductive heat addition and boiling that led to supercritical fluid formation. The inlet fluid composition was varied to represent four different geothermal systems. Experiment #1 (low NaCl) corresponds to a young geothermal system with low NaCl and low volatile contents and water of meteoric origin. Experiment #2 (low NaCl+reacted) is similar in nature as experiment #1 but represents a more mature and reacted geothermal system. Experiment #3 (low NaCl+HCl) and #4 (NaCl+CO_2) relate to the formation of supercritical fluids typical for subduction-related geothermal systems with enriched NaCl concentrations and volatile gas input of either HCl or CO_2.

The experimental set-up used in this study involves flow-through experiments. The inlet solution of known composition is injected by a HPLC pump at a flow rate of <0.2 ml min^{-1} to a reactor that is heated to >400 °C at 69 bars. After passing through the reactor, the solution is eventually cooled down by joined in flow cooling jackets. The pressure of the experiment is regulated by a fixed back pressure regulator. The reactor contains a threaded stainless steel (316) rod to collect mineral deposits precipitating from the solution.

The inlet solutions used for the experiments have been sampled from liquid and two-phase wells from active geothermal fields in Iceland. To simulate supercritical fluids in low-NaCl geothermal system, sampled geothermal water from Spóastaðir (S Iceland) was used to represent a geothermal system at the incipient (young) stage (experiment #1) and a separated liquid from the well KJ-17 (Krafla, NE Iceland) represented a geothermal system at a reacted (mature) stage (experiment #2). Supercritical fluid formation in reacted (mature) geothermal systems involving the contribution of magmatic gases (experiments #3 and #4) was simulated using separated liquid from well KJ-17 spiked with HCl and Na_2CO_3, respectively.

The solid products were collected from inside the reactor and the rod after each experimental run. The loose deposits were mounted on a sample holder to study their morphology. The rod was imbedded in epoxy, cut perpendicular to the flow direction of the solution during the experiment and subsequently polished and carbon-coated. Both, the morphology and secondary mineral phases of the deposits and precipitates along the rod were determined using a HITACHI TM-300 scanning electron microscope (SEM) with an accelerating voltage of 15 kV.

2.2 Geochemical model

The geochemical model involved increase in specific enthalpy of the subcritical fluids at constant temperature and pressure conditions and boiling of the liquid to complete dryness. Calculations were carried out assuming closed-system boiling and reaction of major elements between liquid, vapor and solid phase, allowing saturated minerals to precipitate at each simulated step. To run the simulations, we used PHREEQC geochemical software (version 3.1.2) and WATCH (Bjarnason 2010) programs. Thermodynamic database used in these calculations was llnl.dat (Delany 1991) which was updated with respect to mineral solubility constants (Holland and Powell 1998; Leusbrock et al. 2009; Leusbrock et al. 2010; Holland and Powell 2011; Stefánsson et al. 2011). The redox state of the solution was calculated with aid of PHREEQC using a S^{-2}/S^{6} redox pair. The volatility of other

elements was taken to be negligible. The elements and compounds included in the calculations were Si, B, Na, K, Ca, Mg, Al, Fe, Cl, F, H_2S, SO_4 and CO_2 and respective aqueous and vapor species. The solubility of H_2S and CO_2 were calculated based on Fernández-Fernández-Prini et al. (2003), whereas HF was assumed to enter the vapor phase upon complete boiling. Secondary minerals selected here were those observed at low (<200 °C) and high-temperature (>250 °C) in geothermal systems. The starting solution composition used in the simulations was the same as the inlet solutions used in the experiments.

3. RESULTS

3.1 Experimentally observed secondary minerals and mineral composition

SEM microphotographs showing the main secondary mineralogy are displayed in Figure 2. Selected EDS analysis of the mineral phases are listed in Table 1.

In experiments #1 and #2, the observed mineral deposits were white, with variable thickness (up to 1.5 mm in its maximum). The deposits consisted of <50µm thick dense Ca-rich rim close to the rod, followed by a porous layer of variable thickness (<1 mm) toward the surface, consisting of mostly quartz and silica colloids (amorphous silica), as well as scarce euhedral feldspars up to 0.3 mm in length, semi euhedral crystals of wollastonite. In experiment #1, the composition of wollastonite varied from pure endmember wollastonite ($CaSiO_3$) to wollastonite exhibiting impurities of Na and K. The composition of feldspar corresponded to anorthite ($X_{anorthite}$ = 0.85). In experiment #2, wollastonite also contained impurities of Na and K. The composition of feldspar, however, corresponded to microcline ($X_{microcline}$ = 0.9) with minor amounts of Na and Ca. Quartz was mainly of pure endmember composition with only minor impurities of Ca and Na.

In experiment #3 (low NaCl+HCl), the rod collected after the experiment was heavily corroded and no secondary minerals were found.

The alteration deposits observed in experiment #4 were up to 2 mm thick and revealed highly porous layers close to the rod. These layers consisted of significant amounts of needle-like wollastonite of up to 5 µm length followed by randomly distributed up to 25 µm long crystals of Na-feldspars, salt and quartz with crystals of 5-10 µm in length. This part transitioned into a thin layer of amorphous silica (silica gel structures of diameter less than 1µm). Quartz was of pure endmember composition with a small percentage of Na-impurities. Feldspar was of pure albitic composition (X_{albite} = 0.99). Wollastonite contained minor amount of Na. Salt minerals were mainly composed of halite and small fraction of sylvite.

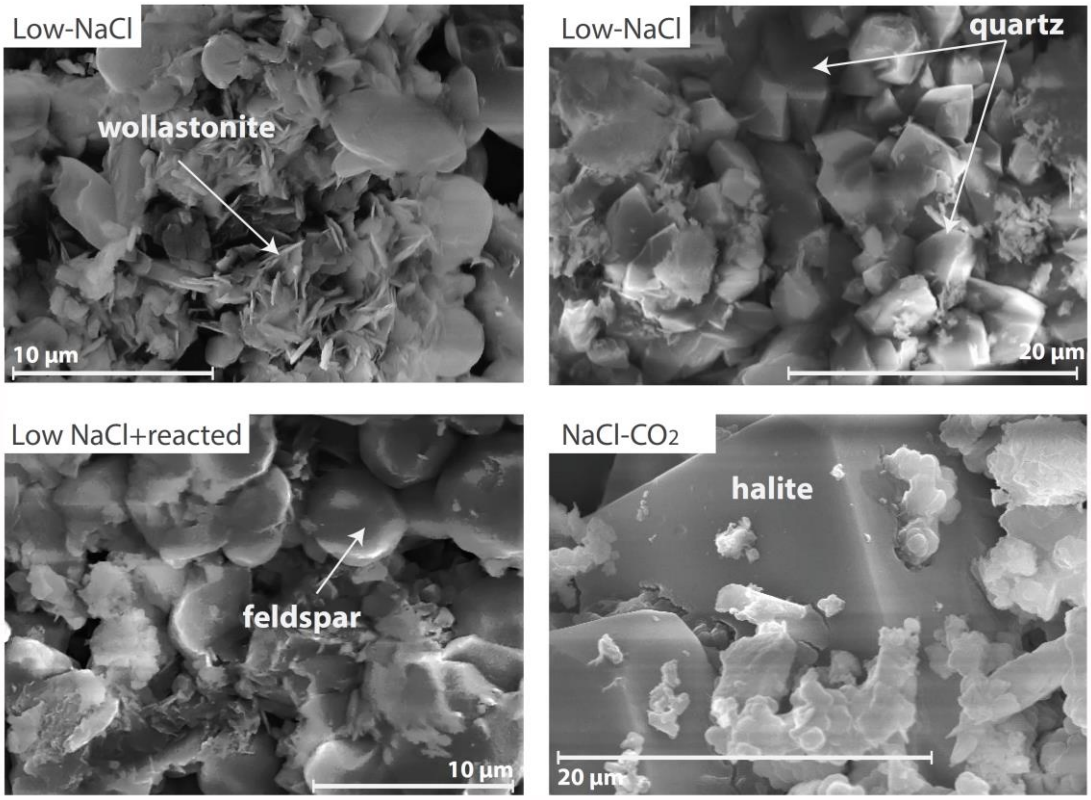

Figure 2: SEM microphotographs of the secondary mineral deposits collected after each experiment.

Table 1: Selected EDS analysis of the mineral deposits collected after the experiments. The concentrations are normalized and presented as wt %.

exp #1 (low NaCl)	quartz	feldspar	wollastonite	Wollastonite
Oxide				
SiO_2	99.4	52.0	49.3	47.0
Al_2O_3	0.00	29.1	3.49	0.00
CaO	0.00	16.4	36.7	53.0
Na_2O	0.632	2.49	10.6	0.00
K_2O	0.00	0.00	0.00	0.00
Total	100	100	100	100
exp# 2 (low NaCl + reacted)	quartz	feldspar	feldspar	Wollastonite
Oxide				
SiO_2	100.0	51.5	56.2	59.5
Al_2O_3	0.00	22.5	18.4	0.0
CaO	0.00	1.26	0.00	25.2
Na_2O	0.00	2.18	4.39	8.64
K_2O	0.00	22.5	21.0	6.64
Total	100	100	100	100
exp#3 ($NaCl+CO_2$)	quartz	feldspar	wollastonite	Halite
Oxide				
SiO_2	80.7	46.1	50.7	0.00
Al_2O_3	0.00	35.4	0.00	0.00
CaO	0.00	0.00	31.2	0.00
Na_2O	19.3	18.5	18.1	49.05
K_2O	0.00	0.00	0.00	0.00
Element				
Cl	0.00	0.00	0.00	50.95
Total	100	100	100	100

3.2 Modeled alteration sequence

The modeled alteration sequence along with associated elemental loss in the fluid phase is presented in Figure 3.

At subcritical conditions (liquid zone), the geothermal fluids in young (immature) geothermal systems were in equilibrium with secondary minerals commonly associated with low-temperature (zeolitic) alteration. Such alteration included calcite, Fe-Mg clays such as saponites or smectites and Ca-Na-zeolites (mordenite, mesolite and stilbite). In the case of a more mature (reacted) geothermal system, geothermal fluids were in equilibrium with epidote, chlorites, (Na-K) feldspar, grossular, pargasite, prehnite and wollastonite. In addition, wairakite, along with prehnite and micas (illite-muscovite) appeared in geothermal systems with elevated NaCl and gas contents.

Upon boiling of the fluid to complete dryness (liquid and vapor zone), the modeled alteration sequence for immature geothermal systems (experiment #1) consisted of silica (chalcedony), zeolites (scolecite), clays (Ca-Na saponites) and salts (halite-sylvite). Accordingly, the boiled fluid composition contained negligible amounts of Si, Mg, Al, Na, K, Ca, while concentrations of C, S and B were comparable with corresponding concentrations of the un-boiled subcritical fluids. In mature geothermal systems (experiment #2), the alteration sequence associated with boiling of geothermal fluids included Mg-chlorites, Na-K feldspar, wollastonite, halite and quartz. Correspondingly, fluid composition reflected elemental loss in Si, Al, Na, K, Mg and Fe concentrations. In geothermal systems with elevated NaCl and gas concentrations (experiments #3 and #4), the alteration included wollastonite, albite-microcline, quartz, and major amounts of halite. As in the previous cases, boiling of $NaCl$-CO_2 rich fluids (experiment #4) resulted in loss of Si, Na, K and Al. However, partitioning of Al into feldspar prevented chlorite precipitation and increased the mobility of Mg and Fe. The remaining Na might eventually precipitate as halite at the final stage of the boiling. Acid addition in form of HCl (experiment #3) resulted in increased solubility of non-volatile (mineral-forming) elements in the liquid phase, whereas silica and (Na,K-Cl) salts were the only minerals precipitating continuously as the boiling proceeded. At supercritical conditions, the resulting fluid composition in all simulated geothermal systems was dominated by CO_2, H_2S and B, whereas concentrations of mineral-forming elements were significantly lower compared to the subcritical (liquid) geothermal reservoir.

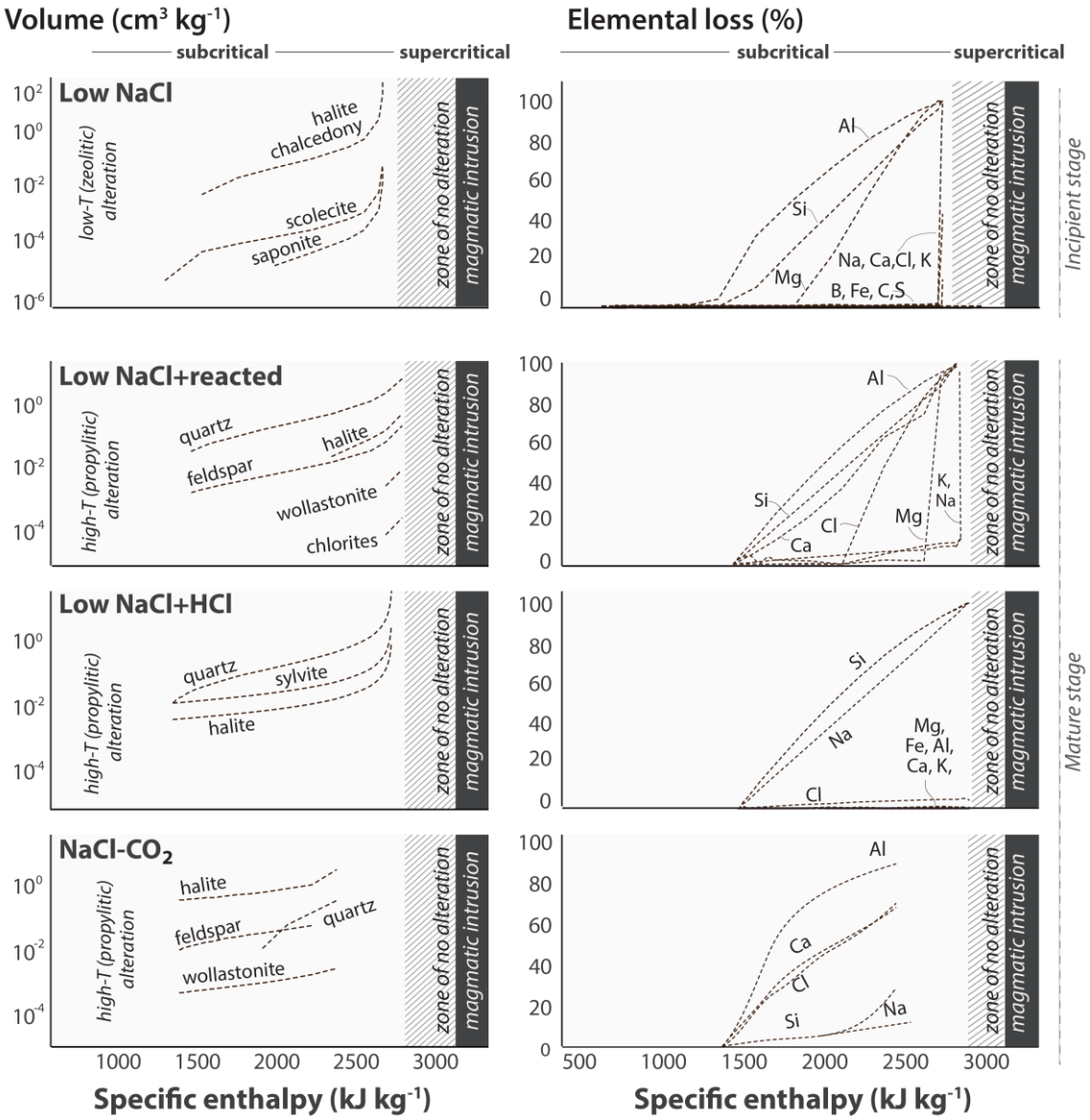

Figure 3: Modeling results of elemental mobility and minerals formed upon supercritical fluid formation in incipient (immature) and mature (reacted) geothermal systems. The liquid zone at subcritical conditions in immature geothermal system is limited by specific enthalpy of 852 kJ kg^{-1}, the liquid and vapor zone by 2792 kJ kg^{-1} and the supercritical fluid zone is defined by >2792 kJ kg^{-1}. In reacted systems, the liquid zone is limited by 1085 kJ kg^{-1}, the liquid and vapor zone by 2801 kJ kg^{-1}, and the supercritical fluid region is defined by specific enthalpy >2801 kJ kg^{-1}.

4. DISCUSSION

4.1 Comparison between experimental and modeled results

As previously shown by Heřmanská et al. (2019), modeled supercritical fluid compositions agree with experimental results and naturally observed fluid compositions. This confirms the hypotheses that supercritical fluids may form by conductive heat transfer into subcritical reservoir and isobaric boiling.

The modeled and experimental secondary mineral sequences for reacted (mature) low NaCl (experiment #2), high NaCl and gas-rich (experiments #3 and #4) geothermal systems are in good agreement. The alteration sequence included silica (quartz), feldspar and wollastonite (experiment #2); salts and quartz (experiment #3) and halite, quartz and feldspar (experiments #4). By volume, silica dominates in NaCl and HCl-rich systems (up to 99.7 % by volume), whereas salts (mostly halite) dominated the alteration sequence in NaCl-CO_2 rich systems (up to 97.0 % by volume). Other mineral groups, such as aluminosilicates and Ca-silicates were only present in traces, which agrees well with the SEM analysis of experimental samples.

Disagreement was found between experimental and modeled results for supercritical fluid formation in immature geothermal systems (experiment #1). The observed experimental secondary mineralogy consisted of quartz, wollastonite and feldspar, which are minerals previously associated with high-temperature systems. In contrast, the modeled mineral sequence consisted of chalcedony, clays and Ca-zeolites. Okamoto et al. (2010) suggested that the precipitated silica morphology and kinetics depend also on fluid composition. Thus, boiling to supercritical conditions of fluids containing significant amounts of Na, K and Al would favor

precipitation of silica in form of Al-silicates and quartz. In contrast, supercritical fluid formation upon boiling of fluids being supersaturated with silica would lead to the precipitation of amorphous silica.

4.2 Controls on secondary mineralogy at the subcritical-supercritical phase boundary

The volume of secondary minerals from each modeled scenario is shown in Figure 3. In all studied scenarios, volume exponentially increased as boiling proceeded towards supercritical conditions. Type and volume of secondary minerals may differ with varying fluid source temperatures, compositions and pH. Increased boiling temperatures may lead to significantly higher volumes of precipitated secondary minerals. As an example, upon boiling of 1kg of subcritical geothermal fluids in immature low NaCl system at boiling temperature <200 °C, at a vapor fraction of 0.5, boiling will yield 0.016 cm^3 of deposits. In case of mature and reacted geothermal systems where the boiling temperatures exceed 250 °C, deposition is twenty times larger (~ 0.3 cm^3). Experimental results also showed that only a fraction of secondary minerals has been deposited within reactor, while the majority of silica precipitated in form of colloids and may have been carried within the flow.

Deposition is also affected by fluid source salinity. In the case of NaCl enriched geothermal systems (experiments #3 and #4) where the NaCl concentration is ~1000 ppm, at a vapor fraction of 0.5, 1kg of boiling fluids produces 1 cm^3 of deposited minerals, which is approximately three times larger than in low NaCl, mature systems. Intuitively, this number may increase as salinity in seawater-dominated systems can be up to 35 times larger than in our modeled scenarios. As the volume of halite per 1 mol is higher than the volume of quartz per 1 mol, presence of saline fluids may enhance precipitation of secondary minerals and induce possible clogging of voids at the magmatic-geothermal contact zone. As boiling proceeds (X_{vapor} > 0.5) the differences in the volume of precipitated minerals between different geothermal systems become smaller.

Influx of magma-derived gases into high-temperature geothermal systems may decrease the pH of the circulating fluid and increase the solubility of Al-silicates. As a result, the alteration sequence formed upon supercritical fluid formation may primarily consist of silica and salts (halite and sylvite). The volume of the deposit is comparable to the other modeled scenarios. However, acid addition may enhance precipitation of silica in form of colloids that are carried within the flow.

4.3 Implications for utilization of fluids formed at the magmatic-geothermal contact zone

Our results suggest that the chemical composition of the subcritical reservoir in geothermal systems has a major impact on the secondary mineralogy associated with formation of supercritical fluid formation at the magmatic-geothermal contact zone. We predict massive precipitation in the zone of supercritical fluid formation, whereas deposition of secondary minerals dramatically decreases in the zone of where only supercritical fluids are present.

Utilization of supercritical fluids from the zone of supercritical fluid formation may lead to scaling within the wells, as previously observed at orifices of the IDDP-1 well in Krafla. In general, the volume of precipitates increases with boiling temperature and salinity of the source fluids.

However, fluids discharged from the upflow zone where supercritical fluids begin to condense contain a similar volatile content compared to the surrounding subcritical fluids. As the concentration of mineral-forming elements is significantly lower, supercritical fluid condensation results in highly acidic character of the condensate that might be responsible for well corrosion. Magmatic degassing may further contribute to the corrosive character of supercritical fluids that may carry silica colloids that precipitate onto the well orifices.

6. CONCLUSIONS

The presence of supercritical fluids results in major permeability changes at the magmatic-geothermal contact zone. The alteration sequence associated with supercritical fluid formation in high-temperature geothermal systems consists of Fe-Mg-Al silicates, Na-K Al silicates, wollastonite and halite. The volume and type of secondary minerals are controlled by reservoir conditions, fluid source composition and magma gas addition to subcritical reservoir fluids. Temperatures at which subcritical liquid fluids begin to boil along with their salinity are the key parameters affecting the volume of deposited secondary minerals. The volume of deposited minerals is predicted to be highest in reacted (mature) geothermal systems supplied with NaCl-rich fluids and higher boiling temperatures (>250 °C). As the volume of secondary mineral deposits increases, host rock permeability decreases, leading to possible deteriorating fluid flow around magmatic intrusion, which may have potential impact on further geothermal system evolution.

Utilization of supercritical fluids from their zones of formation may risk massive precipitation of secondary minerals within the well. Furthermore, geothermal wells may discharge fluids from the upflow zone where supercritical fluid condense and form acid fluids with highly corrosive character.

ACKNOWLEDGEMENTS

We would like to thank Ríkey Kjartansdóttir for her help with chemical analysis and assistance in the lab, and Andri Ísak Þórhallsson, Gylfi Sigurðsson and Magnús Ingi Magnússon (Velvík ehf) for their help with the experimental set-up and technical assistance.

REFERENCES

Bjarnason, J.Ö.: The Chemical Speciation Program WATCH, Version 2.4., Iceland GeoSurvey, Reykjavík (2010).

Delany, J.M., and Lundeen, S.R.: The LLNL thermochemical data base -- revised data and file format for the EQ3/6 package, United States (1991).

Dolejš, D., and Manning, C.E.: Thermodynamic model for mineral solubility in aqueous fluids: theory, calibration and application to model fluid-flow systems, *Geofluids*, **10,** (2010), 20–40.

Fernández-Prini, R., Alvarez, J.L., and Harvey, A.H. Henry's Constants and Vapor–Liquid Distribution Constants for Gaseous Solutes in H_2O and D_2O at High Temperatures, *Journal of Physical and Chemical Reference Data,* **32**, (2003), 903–916.

Fournier, R.O., and Potter, R.W.: An equation correlating the solubility of quartz in water from 25° to 900°C at pressures up to 10,000 bars, *Geochimica et Cosmochimica Acta,* **46,** (1982), 1969–1973.

Friðleifsson, G.Ó., Elders, W., and Albertsson, A.: The concept of the Iceland Deep Drilling Project, *Geothermics,* **49,** (2014), 2–8.

Heřmanská, M., Stefánsson, A., and Scott, S.: Supercritical fluids around magmatic intrusions: IDDP-1 at Krafla, Iceland, *Geothermics,* **78,** (2019), 101–110.

Holland, T.J.B., and Powell, R.: An improved and extended internally consistent thermodynamic dataset for phases of petrological interest, involving a new equation of state for solids, *Journal of Metamorphic Geology,* **29,** (2011), 333–383.

Holland, T.J.B., and Powell, R.: An internally consistent thermodynamic data set for phases of petrological interest, *Journal of Metamorphic Geology,* **16**, (1998), 309–343.

Leusbrock, I., Metz, S.J., Rexwinkel, G., and Versteeg, G.F.: Solubility of 1:1 Alkali Nitrates and Chlorides in Near-Critical and Supercritical Water, *Journal of Chemical and Engineering Data,* **54**, (2009), 3215–3223.

Leusbrock, I., Metz, S.J., Rexwinkel, G., and Versteeg, G.F.: The solubility of magnesium chloride and calcium chloride in near-critical and supercritical water, *Journal of Supercritical Fluids,* **53**, (2010), 17–24.

Manning, C.E.: The solubility of quartz in H_2O in the lower crust and upper mantle, *Geochimica et Cosmochimica Acta,* **58,** (1994), 4831–4839.

Rivera-Diaz, A., Kaya, E., and Zarrouk, S.J.: Reinjection in geothermal fields − A worldwide review update, *Renewable and Sustainable Energy Reviews,* **53,** (2016), 105–162.

Scott, S., Driesner, T., and Weis, P.: Geologic controls on supercritical geothermal resources above magmatic intrusions, *Nature Communications,* **6**, (2015).

Scott, S., Driesner, T., and Weis, P.: The thermal structure and temporal evolution of high-enthalpy geothermal systems, *Geothermics,* **62**, (2016), 33–47.

Simonson, J.M., and Palmer, D.A.: Liquid-vapor partitioning of HCl(aq) to 350°C, *Geochimica et Cosmochimica Acta,* 57, (1993), 1–7.

Stefánsson, A., Arnórsson, S., Gunnarsson, I., Kaasalainen, H., and Gunnlaugsson, E.: The geochemistry and sequestration of H_2S into the geothermal system at Hellisheidi, Iceland, *Journal of Volcanology and Geothermal Research,* **202**, (2011), 179–188.

Stimac, J., Goff, F., and Goff, C.J.: Intrusion-Related Geothermal Systems, in Sigurdsson, H., Houghton, B., McNutt, S., Rymer, H., and Stix, J. (editors): The Encyclopedia of Volcanoes, 377–393, Elsevier, Boston (2015).